Index Terms–**Reentry vehicles, tracking with prescribed performance, funnel control, maneuvering trajectory tracking**

Maneuvering tracking algorithm for reentry vehicles with guaranteed prescribed performance

ZONGYI GUO, Member, IEEE
Institute of Precision Guidance and Control, Northwestern Polytechnical University, Xi'an, China

XIYU GU
Department of Information Engineering, University of Padova, Padova, Italy

YONGLIN HAN
JIANGUO GUO
Institute of Precision Guidance and Control, Northwestern Polytechnical University, Xi'an, China

THOMAS BERGER
Institut für Mathematik, Universität Paderborn, Germany

Abstract— **This paper presents a prescribed performance-based tracking control strategy for the atmospheric reentry flight of space vehicles subject to rapid maneuvers during flight mission. Although earlier works presented control algorithms with a focus on the transient performance, it is still an open problem how to ensure the stability of the system during maneuvering flight missions. A time-triggered non-monotonic performance funnel is proposed with the aim of constraints violation avoidance in the case of sudden changes of the reference trajectory. Compared with traditional prescribed performance control methods, the proposed funnel boundary is adaptive with respect to the reference path and is capable of achieving stability under disturbances. A recursive control structure with low complexity is introduced which does not require any knowledge of specific system parameters. By a stability analysis we show that the tracking error evolves within the prescribed error margin under a condition which represents a trade-off between the reference signal and the performance funnel. The effectiveness and robustness of the proposed control scheme is verified by simulations.**

Z. Guo, Y. Han, and J. Guo are with the Institute of Precision Guidance, and Control, Northwestern Polytechnical University, Xi'an 710072, China, (e-mail: guozongyi@nwpu.edu.cn; hanyonglin@mail.nwpu.edu.cn; guojianguo@nwpu.edu.cn). X. Gu is with Department of Information Engineering, University of Padova, Padova, Italy, (xiyu.gu@studenti.unipd.it). T. Berger is with the Universität Paderborn, Institut für Mathematik, Warburger Str. 100, 33098 Paderborn, Germany, (thomas.berger@math.upb.de). (Corresponding author: Xiyu Gu.)

This work was supported by the National Natural Science Foundation of China under Grant 92271109 and Grant 52272404 and the Deutsche Forschungsgemeinschaft (DFG, German Research Foundation) under Project-IDs 362536361 and 471539468.

I. INTRODUCTION

For the cost efficiency of space missions it is imperative that spacecrafts are able to return to earth through its atmosphere, following a prescribed trajectory. Such atmospheric reentry problems are a main focus of the aerospace industry and have received a large amount of attention during the last decade. Trajectory tracking strategies for reentry vehicles (RVs) have long been considered as a hot research area, owing to their unique attributes, which include high flight velocities, rapid response times, and expansive operational capabilities [1]-[4]. Maneuvering flight, as one branch of such atmospheric reentry problems, has stimulated extensive research in the areas of evasion, pursuit and obstacle avoidance for missions achievement [5]-[8]. Commonly, the main objective of maneuvering flight control is stability and robustness of the system and to provide the stabilization capabilities in RV tracking either on-line or for off-line planned reference trajectories. Some widespread control approaches, including PID [9], sliding mode control [10], backstepping control [11], adaptive control [12], [13], optimization algorithms [14], [15] and intelligent algorithms [16], [17], are the popular choice owing to their simplicity and effectiveness in RV tracking problems. The aforementioned conventional control methods for trajectory tracking primarily center on ensuring system stability, often overlooking the crucial influence of transient performance on the final outcomes. Those results demonstrated that the tracking objective can be successfully accomplished, whereas, it remains an open issue how to guarantee its high speed convergence, minimum accuracy and small overshoot. Consequently, there is a compelling need to delve into the research of transient issues within the domain of trajectory tracking for RVs, in order to ensure a successful mission.

Control algorithms for constraining the transient performance are flourishing during the past few decades, and two different approaches have been developed. Prescribed performance control (PPC) has been proposed in [18]-[20] and is regarded as a representative nowadays. It relies on an error transformation, which is designed to transform the original output error restrictions into an equivalent interval one. Since its universal control structure, PPC has been thoroughly investigated in combination with unconstrained control methods like backstepping and sliding mode control. Funnel control (FC) is the second control mechanism for guaranteeing a prescribed performance of the tracking error [21]-[25] by introducing a time-varying high-gain feedback in the control law. If the error tends towards the funnel boundary, the gain increases so that the error is kept inside the performance funnel. Notice that almost all funnel boundaries selected in works on funnel control are monotonically decreasing functions, although the theory guarantees the stability of the closed-

loop system for a vast variety of non-monotonic funnel boundaries. It turns out that for flight maneuvering, non-monotonic funnel boundaries are more suitable. However, sudden flight maneuvers may lead to a drastic increase of the control effort or even drive the tracking error across the funnel boundary, resulting in closed-loop system instability. Although both PPC and FC have already been investigated for the control algorithm design for RVs with a focus on the transient performance [26]-[28], how to ensure the stability of the system during maneuvering flight is still an open question.

Considering the various demands of trajectory tracking for RVs during different phases, a control law which adapts itself to the prescribed boundary function is required to guarantee the transient behavior in flight maneuvering. Therefore, a time triggered non-monotonic funnel boundary is proposed in this paper. Using a priori information of the reference trajectory, we design a boundary function which is widened during critical phases, e.g. in the case of sudden course corrections. In this way, peaks in the control input signal are avoided. Additionally, disturbances (such as noises, uncertainties or unmodeled dynamics) are taken into account, as they might have a detrimental effect on the system's performance. A significant challenge in stability analysis is imposed by the dynamics of the RV, where the flight lateral position (which is the system output) is influenced by the deflection angle only in a saturated way (via a $\sin$ function). Therefore, arbitrary instantaneous changes of the lateral position are not possible. Any prescribed trajectory can only be tracked up to a certain accuracy, i.e., there is a trade-off between the derivative of the reference and the funnel boundary function. To the best of our knowledge, this is the first work where such a trade-off is found for RV tracking problems with guaranteed prescribed performance.

Focusing on the issues mentioned above, the main contributions of this paper are summarized as follows.

- We design a robust funnel control law with time triggered non-monotonic funnel boundary for flight maneuvering with guaranteed transient performance under disturbances. Compared to [26], the proposed recursive funnel control structure is of low complexity and avoids the requirement of a priori knowledge of the system parameters.

- For maneuvering trajectory tracking, we derive a condition representing a trade-off between the reference trajectory and the funnel boundaries, under which the RV is amenable to the proposed funnel control law.

The remainder of this paper is organized as follows. The dynamic model of the RV in yaw channel is presented in Section II, together with the proposed funnel boundary and the control objective. In Section III we state the funnel-based control law design and provide the stability analysis. Simulation results are given in Section IV and Section V finally concludes this article.

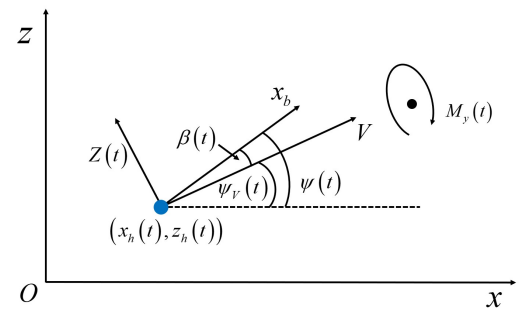

Fig. 1. Engagement geometry and parameter definitions.

II. PROBLEM FORMULATION

A. RV Dynamics

Considering horizontal lateral maneuvers with constant velocity, the engagement geometry and parameter definitions of a RV are shown in Fig. 1, where the xz-plane is the projection of the ground coordinate system to the horizontal plane, and x_b is the vector from the centroid of the RV to its head. The simplified model of the RV in yaw channel is established in [29], [30] as

$$\dot{z}_h(t) = -V\sin(\psi_V(t)) + \Delta_0(t) \tag{1}$$

$$\dot{\psi}_V(t) = -\frac{1}{mV}Z(t) + \Delta_1(t) \tag{2}$$

$$\dot{\psi}(t) = \omega_y(t) + \Delta_2(t) \tag{3}$$

$$\dot{\omega}_y(t) = \frac{M_y(t)}{J_y} + \Delta_3(t) \tag{4}$$

$$\beta(t) = \psi(t) - \psi_V(t) \tag{5}$$

where $z_h(t)$ is the flight altitude, m is the mass, V is the flight speed, ψ_V, ψ, β represent the deflection angle, yaw angle and sideslip angle, ω_y is the yaw rate, J_y denotes the yaw rotational inertia and Δ_i $(i = 0,1,2,3)$ are bounded disturbances. The functions Z and M_y are the aerodynamic force and moment in yaw channel, expressed by $Z(t) = \bar{q}S(c_z^{\alpha}\alpha + c_z^{\beta}\beta(t) + c_z^0)$, $M_y(t) = \bar{q}Sl(c_M^{\alpha}\alpha + c_M^{\beta}\beta(t) + c_M^{\delta_y}\delta_y(t) + c_M^0)$, where α is the angle of attack, δ_y represents the rudder angle, $\bar{q}$ is the dynamic pressure, S and l are the reference area and aerodynamic chord of the RV, and c_z^i and c_M^j $(i = \alpha,\beta,0, j = \alpha,\beta,\delta_y,0)$ are the aerodynamic coefficients for force and moment, respectively. The rudder angle δ_y can be manipulated and serves as the control input.

Note that in this paper, we focus on lateral maneuvering and do not intervene in the transverse movement of the aircraft along the x-axis. In this framework, although the dynamics of the position component x_h of the RV (also depicted in Fig. 1) are given by $\dot{x}_h(t) = V\cos(\psi_V(t))$, x_h does not influence the other state variables in (1)–(5), hence those dynamics can be ignored. Then we introduce the variables $y_0(t) = z_h(t)$, $y_1(t) = \psi_V(t)$, $y_2(t) = \beta(t) = \psi(t) - \psi_V(t)$, $y_3(t) =$

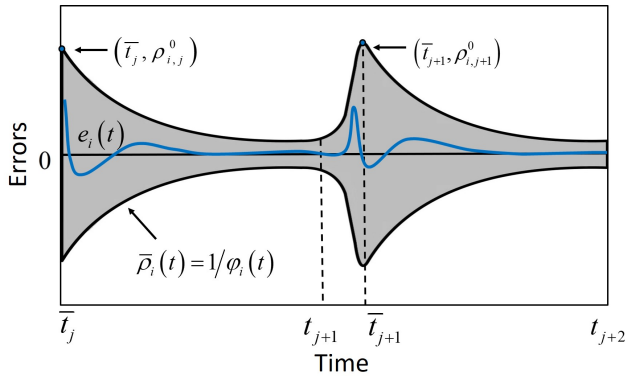

Fig. 2. Tracking error evolution in the funnel $\Gamma_{\varphi_i} (i = 0, 1, 2, 3)$.

$\omega_y(t)$ and the control input $u(t) = \delta_y(t)$ to rewrite the dynamic model (1)–(5) in the form

$$\dot{y}_0(t) = -V \sin(y_1(t)) + \Delta_0(t) \tag{6}$$
$$\dot{y}_1(t) = -c_1 - c_2 y_2(t) + \Delta_1(t) \tag{7}$$
$$\dot{y}_2(t) = y_3(t) + c_1 + c_2 y_2(t) + \Delta_2(t) - \Delta_1(t) \tag{8}$$
$$\dot{y}_3(t) = c_3 + c_4 y_2(t) + c_5 u(t) + \Delta_3(t) \tag{9}$$

with the constants $c_1 = \frac{1}{mV}\bar{q}S\left(c_z^\alpha \alpha + c_z^0\right)$, $c_2 = \frac{1}{mV}\bar{q}Sc_z^\beta$, $c_3 = \frac{1}{J_y}\bar{q}Sl\left(c_M^\alpha \alpha + c_M^0\right)$, $c_4 = \frac{1}{J_y}\bar{q}Sc_M^\beta$, $c_5 = \frac{1}{J_y}\bar{q}Sc_M^{\delta_y}$.

It can be seen from the dynamics (1) that the flight altitude z_h is influenced only by the deflection angle ψ_V and that this influence is saturated by the sin function. Therefore, it is clear that it is impossible to achieve tracking of arbitrary reference signals with arbitrary prescribed performance. There must be a trade-off between the reference signal ($\dot{z}_{h_{ref}}$) and the funnel boundary. This trade-off is formulated as condition (15) in Theorem 1.

B. Funnel Boundary

We define functions $\varphi_i(t)$ $(i = 0, 1, 2, 3)$ as the reciprocal of the funnel boundary $\bar{\rho}_i(t)$, which describe the performance funnel Γ_{φ_i} (cf. [21]) as

$$\Gamma_{\varphi_i} := \{(t, e_i) \in \mathbb{R}_{\geq 0} \times \mathbb{R} \mid \varphi_i(t)|e_i(t)| < 1\}. \tag{10}$$

The functions $\varphi_i(t)$ are continuously differentiable, bounded with bounded derivatives, and satisfy $\varphi_i(t) > 0$ for all $t \geq 0$ and $\liminf_{t\to\infty} \varphi_i(t) > 0$. Fig. 2 displays the reciprocal $\bar{\rho}_i(t) = 1/\varphi_i(t)$.

In order to avoid peaks in the control input signal due to a strongly varying reference trajectory, we employ a non-monotonic funnel boundary defined as

$$1/\varphi_i(t) = \bar{\rho}_i(t) = \begin{cases} \bar{\rho}_{i,0}(t) & 0 \leq t < t_1 \\ a_{i,0}(t-t_1)^3 + b_{i,0}(t-t_1)^2 + c_{i,0}(t-t_1) + d_{i,0} & t_1 \leq t < \bar{t}_1 \\ \bar{\rho}_{i,1}(t) & \bar{t}_1 \leq t < t_2 \\ \vdots & \vdots \\ a_{i,j-1}(t-t_j)^3 + b_{i,j-1}(t-t_j)^2 + c_{i,j-1}(t-t_j) + d_{i,j-1} & t_j \leq t < \bar{t}_j \\ \bar{\rho}_{i,j}(t) & \bar{t}_j \leq t < t_{j+1} \\ \vdots & \vdots \\ a_{i,p-1}(t-t_p)^3 + b_{i,p-1}(t-t_p)^2 + c_{i,p-1}(t-t_p) + d_{i,p-1} & t_p \leq t < \bar{t}_p \\ \bar{\rho}_{i,p}(t) & \bar{t}_p \leq t \end{cases} \tag{11}$$

where t_j and $\bar{t}_j$ $(j = 1, ..., p)$ are the triggered time and initial time points of every phase after maneuvering, $\bar{t}_j - t_j$ is the time range for maneuvering and p represents the number of triggered times. The polynomials in each interval of the form $[t_j, \bar{t}_j]$ are chosen based on the current maneuver encoded in the reference trajectory, and they ensure a widening of the funnel boundary. The functions $\bar{\rho}_{i,j}(t)$ $(i = 0, 1, 2, 3, j = 1, 2, ..., p)$ are of the form

$$\bar{\rho}_{i,j}(t) = \left(\rho^0_{i,j} - \rho^\infty_{i,j}\right) e^{-l_{i,j}t} + \rho^\infty_{i,j} \tag{12}$$

with initial funnel width $\rho^0_{i,j} > 0$, required minimum exponential convergence rate $l_{i,j} > 0$ and the maximum steady state error $\rho^\infty_{i,j} > 0$, respectively. In order to guarantee that $\bar{\rho}_i$ is continuously differentiable, the parameters $a_{i,j}, b_{i,j}, c_{i,j}, d_{i,j}$ are chosen such that $\lim_{t\to t_j^-} \bar{\rho}_i(t) = \lim_{t\to t_j^+} \bar{\rho}_i(t)$, $\lim_{t\to \bar{t}_j^-} \bar{\rho}_i(t) = \lim_{t\to \bar{t}_j^+} \bar{\rho}_i(t)$, $\lim_{t\to t_j^-} \dot{\bar{\rho}}_i(t) = \lim_{t\to t_j^+} \dot{\bar{\rho}}_i(t)$, $\lim_{t\to \bar{t}_j^-} \dot{\bar{\rho}}_i(t) = \lim_{t\to \bar{t}_j^+} \dot{\bar{\rho}}_i(t)$ for $j = 1, \ldots, p$.

The proposed funnel boundary is displayed in Fig. 2 and we stress that it is different from the monotonically decreasing boundary functions of the form (12) widely used in [20], [22], [25]. Instead, it is a time triggered mechanism with trigger time points t_j, chosen in accordance with the reference trajectory, so that the proposed funnel (11) adapts itself and is suitable for the time-varying maneuvering command of RVs. For $t > t_p$ the proposed funnel boundary converges to a neighbourhood of the origin, satisfying $\lim_{t\to\infty} \bar{\rho}_i(t) = \rho^\infty_{i,p} > 0$.

C. Control Objective

The control objective is to design an output derivative feedback such that for any sufficiently smooth reference trajectory $z_{h_{ref}}$, any initial values and under the influence of disturbances, the tracking error $z_h - z_{h_{ref}}$ evolves within a prescribed performance funnel Γ_{φ_0} as in (10) and hence exhibits the desired transient and steady behavior. Furthermore, all signals u, z_h, ψ_V, ψ, β and ω_y in the closed-loop system should remain bounded.

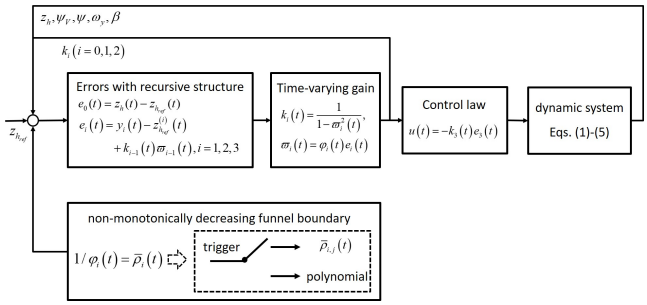

Fig. 3. Funnel control structure for RV tracking issue.

III. FUNNEL CONTROLLER DESIGN

A. Funnel-based control law design

Before we define the control law we introduce the following assumptions.

ASSUMPTION 1. *The reference trajectory $z_{h_{ref}}$ is known, it is four times continuously differentiable and its first four derivatives are bounded.*

ASSUMPTION 2. *The disturbances Δ_i are measurable and essentially bounded with $\|\Delta_i\|_\infty \leq D_i$ for known constants $D_i \geq 0$ $(i=0,1,2,3)$.*

Assumptions 1 and 2 are reasonable and frequently used in the literature. The disturbances Δ_i $(i=0,1,2,3)$ involved in (1)-(5) account for uncertainties in the aerodynamic coefficients, noises and external disturbances, which are usually bounded throughout the flight process.

We define the tracking error as

$$e_0(t) = y_0(t) - z_{h_{ref}}(t) = z_h(t) - z_{h_{ref}}(t)$$

and introduce the following recursive structure

$$e_i(t) = y_i(t) - z_{h_{ref}}^{(i)}(t) + k_{i-1}(t)\,\varpi_{i-1}(t)\,,\ \ i=1,2,3 \tag{13}$$

where $k_i(t) = \frac{1}{1-\varpi_i^2(t)}$ and $\varpi_i(t) = \varphi_i(t)\,e_i(t)$ for φ_i as in (11).

Then the funnel-based control law is given by

$$u(t) = -k_3(t)\,e_3(t) = -\frac{e_3(t)}{1-\varphi_3^2(t)\,e_3^2(t)} \tag{14}$$

and the block diagram of the proposed control scheme is shown in Fig. 3. In the sequel we investigate existence of solutions of the initial value problem resulting from the application of the funnel controller (14) to the RV with dynamics (1)-(5). By a solution of (1)-(5), (14) we mean a function $(z_h, \psi_V, \psi, \omega_y) : [0, t_f) \to \mathbb{R}^4$, $t_f \in (0, \infty]$, which is locally absolutely continuous and satisfies the initial conditions as well as the differential equations (1)-(5) for almost all $t \in [0, t_f)$. A solution is called maximal, if it has no right extension that is also a solution.

B. Stability Analysis

In this part, we present the stability analysis of the proposed control law.

THEOREM 1. *Consider a RV with dynamics (1)-(5), satisfying Assumptions 1-2, under the funnel control law (14). Choose funnel boundaries φ_i $(i=0,1,2,3)$ as in (11) such that the initial values satisfy*

$$\varphi_i(0)|e_i(0)| < 1 \quad (i=0,1,2,3).$$

Additionally, assume that the functions φ_0, φ_1 and $z_{h_{ref}}$ satisfy the following condition:

$$\exists\,\mu \in (0,1)\ \forall\, t \geq 0: \\ \frac{|\dot{\varphi}_0(t)|}{V\varphi_0^2(t)} + \frac{1}{\varphi_1(t)} + \frac{D_0}{V} + \frac{(1+V)}{V}|\dot{z}_{h_{ref}}(t)| \leq \mu. \tag{15}$$

Then the funnel controller (14) applied to (1)-(5) yields an initial-value problem which has a solution, every solution can be maximally extended and every maximal solution $(z_h, \psi_V, \psi, \omega_y) : [0, t_f) \to \mathbb{R}^4$, $t_f \in (0, \infty]$ has the following properties:

- *global existence: $t_f = \infty$;*
- *all errors evolve uniformly in the respective prescribed performance funnels, that is for all $i = 0,1,2,3$ there exists $\varepsilon_i \in (0,1)$ such that for all $t \geq 0$ we have $|\varpi_i(t)| \leq \varepsilon_i$.*
- *all signals z_h, ψ_V, ψ, ω_y, δ_y and k_i $(i=0,1,2,3)$ in the closed-loop system are bounded.*

Proof:
Before the analysis, we record that it follows from (6)-(9) that the derivatives of $e_i(t)$ $(i=0,1,2,3)$ can be expressed as

$$\dot{e}_0(t) = -V\sin(y_1(t)) - \dot{z}_{h_{ref}}(t) + \Delta_0(t) \tag{16}$$

$$\dot{e}_1(t) = e_2(t) - k_1(t)\,\varpi_1(t) + \frac{d}{dt}(k_0(t)\,\varpi_0(t)) \\ -(1+c_2)y_2(t) - c_1 + \Delta_1(t) \tag{17}$$

$$\dot{e}_2(t) = e_3(t) - k_2(t)\,\varpi_2(t) + \frac{d}{dt}(k_1(t)\,\varpi_1(t)) \\ + c_1 + c_2 y_2(t) + \Delta_2(t) - \Delta_1(t) \tag{18}$$

$$\dot{e}_3(t) = c_5 u(t) - z_{h_{ref}}^{(4)}(t) + \frac{d}{dt}(k_2(t)\,\varpi_2(t)) \\ + c_3 + c_4 y_2(t) + \Delta_3(t) \tag{19}$$

In the following, we will first show that a local solution exists on $[0, t_f)$ and the tracking error evolves uniformly within the prescribed performance funnel, and we show $t_f = \infty$ in the last step.

Step 1: To show existence of a solution of the closed-loop system, consider the functions

$$\tilde{e}_0 : D_0 \to \mathbb{R},\ (t, y_0) \mapsto y_0 - z_{h_{ref}}(t) \tag{20}$$

with the set $D_0 := \mathbb{R}_{\geq 0} \times \mathbb{R}$ and

$$\tilde{e}_i : D_i \to \mathbb{R},\ (t, y_0, \ldots, y_i) \mapsto y_i - z_{h_{ref}}^{(i)}(t) \\ + \frac{\varphi_{i-1}(t)\tilde{e}_{i-1}(t, y_0, \ldots, y_{i-1})}{1-\varphi_{i-1}^2(t)\tilde{e}_{i-1}^2(t, y_0, \ldots, y_{i-1})} \tag{21}$$

with the sets

$$\begin{aligned} D_i &:= \{(t, y_0, \dots, y_i) \in D_{i-1} \times \mathbb{R} \mid \\ &\quad \varphi_{i-1}(t)|\tilde{e}_{i-1}(t, y_0, \dots, y_i)| < 1\}, \ (i = 1, 2, 3), \\ D_4 &:= \{(t, y_0, \dots, y_3) \in D_3 \mid \\ &\quad \varphi_3(t)|\tilde{e}_3(t, y_0, \dots, y_3)| < 1\}. \end{aligned} \tag{22}$$

Introducing $Y(t) = (y_0(t), \dots, y_3(t))^\top$ and the function

$$\begin{aligned} &F : D_4 \to \mathbb{R}^4, \ (t, y_0, \dots, y_3) \\ &\mapsto \begin{pmatrix} -V\sin(y_1) + \Delta_0(t) \\ -c_1 - c_2 y_2 + \Delta_1(t) \\ y_3 + c_1 + c_2 y_2 + \Delta_2(t) - \Delta_1(t) \\ c_3 + c_4 y_2 + \Delta_3(t) - c_5 \frac{\varphi_3(t)\tilde{e}_3(t, y_0, \dots, y_3)}{1 - \varphi_3^2(t)\tilde{e}_3^2(t, y_0, \dots, y_3)} \end{pmatrix} \end{aligned} \tag{23}$$

the closed-loop system takes the form

$$\dot{Y}(t) = F(t, Y(t)), \quad Y(0) = (y_0^0, \dots, y_3^0)^\top. \tag{24}$$

Since $(0, Y(0)) \in D_4$ and F is measurable in t, continuous in $(y_0, \dots, y_3)$ and locally essentially bounded, an application of Theorem B.1 from [31] yields the existence of a solution and every solution can be extended to a maximal solution $Y : [0, t_f) \to \mathbb{R}^4$ with $t_f \in (0, \infty]$. Furthermore, the graph of Y is not a compact subset of D_4.

Step 2: We show that k_0 is bounded on $[0, t_f)$. According to the definition of $\varpi_0(t)$ and (16) we have

$$\begin{aligned} \dot{\varpi}_0(t) &= \frac{\dot{\varphi}_0(t)}{\varphi_0(t)}\varpi_0(t) - \varphi_0(t) V \sin(y_1(t)) \\ &\quad + \varphi_0(t)\left(\Delta_0(t) - \dot{z}_{h_{ref}}(t)\right). \end{aligned} \tag{25}$$

By the mean value theorem, for each $t \in [0, t_f)$, there exists $\xi(t)$ between $-k_0(t)\varpi_0(t)$ and $-k_0(t)\varpi_0(t) + e_1(t) + \dot{z}_{h_{ref}}(t)$ such that

$$\begin{aligned} \sin(y_1(t)) &= \sin\left(-k_0(t)\varpi_0(t) + e_1(t) + \dot{z}_{h_{ref}}(t)\right) \\ &= \sin(-k_0(t)\varpi_0(t)) \\ &\quad + \left(e_1(t) + \dot{z}_{h_{ref}}(t)\right)\cos(\xi(t)). \end{aligned} \tag{26}$$

Now define $U_0(t) = \frac{1}{2}\varpi_0^2(t)$, then from (15), (25) and (26), and invoking $|\varpi_0(t)| < 1$ and $|e_1(t)| < 1/\varphi_1(t)$, we find that

$$\begin{aligned} \dot{U}_0(t) &= \varpi_0(t)\dot{\varpi}_0(t) \\ &= \frac{\dot{\varphi}_0(t)}{\varphi_0(t)}\varpi_0^2(t) + \varphi_0(t)\varpi_0(t)(-V\sin(-k_0(t)\varpi_0(t)) \\ &\quad - V(e_1(t) + \dot{z}_{h_{ref}}(t))\cos(\xi(t)) + \Delta_0(t) - \dot{z}_{h_{ref}}(t)) \\ &\le -V\varphi_0(t)\sin(-k_0(t)\varpi_0(t))\varpi_0(t) + \frac{|\dot{\varphi}_0(t)|}{\varphi_0(t)} \\ &\quad + V\varphi_0(t)\left(\frac{1}{\varphi_1(t)} + \frac{D_0}{V} + \frac{(1+V)}{V}|\dot{z}_{h_{ref}}(t)|\right) \\ &\le V\varphi_0(t)(-N(-\varpi_0(t)) + \mu) \end{aligned} \tag{27}$$

where $N : (-1, 1) \to (-1, 1), \ s \mapsto \sin\left(\frac{s}{1-s^2}\right)s$. The function N is symmetric and satisfies $N(-s) = N(s)$.

Choose $\varepsilon_0 \in (0, 1)$ such that $|\varpi_0(0)| < \varepsilon_0$ and $N(\varepsilon_0) < -\mu$. In the following, we show that $|\varpi_0(t)| \le \varepsilon_0$ for all $t \in [0, t_f)$. Assume there exists some $t \in [0, t_f)$ with $|\varpi_0(t)| > \varepsilon_0$ and define

$$\bar{t}_0 := \inf\{t \in [0, t_f) \mid |\varpi_0(t)| > \varepsilon_0\} > 0.$$

Since N is continuous there exists $\eta > 0$ such that $N(s) \le -\mu$ for all $s \in \mathbb{R}$ with $|s - \varepsilon_0| \le \eta$. By symmetry of N we also have $N(s) \le -\mu$ for all $s \in \mathbb{R}$ with $|s + \varepsilon_0| \le \eta$. Since ϖ_0 is continuous with $|\varpi_0(\bar{t}_0)| = \varepsilon_0$, there exists $\bar{t}_1 \in (\bar{t}_0, t_f)$ such that $|\varpi_0(t)| > \varepsilon_0$ and $|\varpi_0(\bar{t}_0) - \varpi_0(t)| < \eta$ for all $t \in (\bar{t}_0, \bar{t}_1]$.

Let $\sigma = \operatorname{sgn}\varpi_0(\bar{t}_0)$, then $\varpi_0(\bar{t}_0) = \sigma|\varpi_0(\bar{t}_0)| = \sigma\varepsilon_0$ and hence $|\varpi_0(t) - \varpi_0(\bar{t}_0)| = |\varpi_0(t) - \sigma\varepsilon_0| \le \eta$ for all $t \in [\bar{t}_0, \bar{t}_1]$. It follows that $N(\varpi_0(t)) \le -\mu$ for all $t \in [\bar{t}_0, \bar{t}_1]$, and hence $\dot{U}_0(t) \le V\varphi_0(t)\big(N(\varpi_0(t)) + \mu\big) \le 0$, which upon integration gives $\varepsilon_0^2 = \varpi_0(\bar{t}_0)^2 \ge \varpi_0(\bar{t}_1)^2 > \varepsilon_0^2$, a contradiction. Hence, $|\varpi_0(t)| \le \varepsilon_0$ for all $t \in [0, t_f)$ and thus k_0 is bounded on $[0, t_f)$.

Step 3: We show that k_1 is bounded on $[0, t_f)$. A standard procedure in funnel control is used by seeking a contradiction. For some $\varepsilon_1 \in (0, 1)$, which we will determine later, suppose that there exists $t_1^* \in [0, t_f)$ such that $\varpi_1(t_1^*) > \varepsilon_1$ and define

$$t_0^* := \max\{t \in [0, t_1^*) \mid \varpi_1(t) = \varepsilon_1\}.$$

Then we find that

$$\forall\, t \in [t_0^*, t_1^*] : \ \varpi_1(t) \ge \varepsilon_1 \tag{28}$$

and hence

$$\forall\, t \in [t_0^*, t_1^*] : \ k_1(t) = \frac{1}{1 - \varpi_1^2(t)} \ge \frac{1}{1 - \varepsilon_1^2}. \tag{29}$$

Define $U_1(t) = \frac{1}{2}\varpi_1^2(t)$, then according to (17) we have

$$\begin{aligned} \dot{U}_1(t) &= \varpi_1(t)\dot{\varpi}_1(t) \\ &= \varpi_1(t)(\dot{\varphi}_1(t)e_1(t) + \varphi_1(t)\dot{e}_1(t)) \\ &= \frac{\dot{\varphi}_1(t)}{\varphi_1(t)}\varpi_1^2(t) - \varphi_1(t)k_1(t)\varpi_1^2(t) - c_1\varphi_1(t)\varpi_1(t) \\ &\quad + \varphi_1(t)\varpi_1(t)(-c_2 y_2(t) + \Delta_1(t) + e_2(t) - y_2(t)) \\ &\quad + \varphi_1(t)\varpi_1(t)\left(1 + 2\varpi_0^2(t)k_0(t)\right)k_0(t)\dot{\varpi}_0(t). \end{aligned} \tag{30}$$

From Step 2 we have that k_0 is bounded on $t \in [0, t_f)$. Furthermore, $\dot{\varpi}_0$ is bounded by (25), $|e_2(t)| < 1/\varphi_2(t)$ and $y_2, \Delta_1, \varphi_1, \dot{\varphi}_1$ are clearly bounded as well, hence there exists an upper bound $C_1 > 0$ such that for all $t \in [0, t_f)$ we have

$$\begin{aligned} &\frac{|\dot{\varphi}_1(t)|}{\varphi_1^2(t)} + c_1 + (1 + c_2)|y_2(t)| + |\Delta_1(t)| + |e_2(t)| \\ &+ \left(1 + 2\varpi_0^2(t)k_0(t)\right)k_0(t)\dot{\varpi}_0(t) \le C_1. \end{aligned} \tag{31}$$

Invoking $|\varpi_1(t)| < 1$ we thus obtain

$$\dot{U}_1(t) \le \varphi_1(t)|\varpi_1(t)|(-k_1(t)|\varpi_1(t)| + C_1) \le 0 \tag{32}$$

when we choose $\varepsilon_1 \in (0, 1)$ large enough so that $\frac{\varepsilon_1}{1-\varepsilon_1^2} \ge C_1$. Upon integration over $[t_0^*, t_1^*]$ we find that

$$\varepsilon_1^2 = \omega_1(t_0^*)^2 \ge \omega_1(t_1^*)^2 > \varepsilon_1^2, \tag{33}$$

a contradiction. Hence $|\varpi_1(t)| \le \varepsilon_1$ for all $t \in [0, t_f)$, and thus k_1 is bounded on $[0, t_f)$.

Step 4: We prove that k_2 is bounded on $[0, t_f)$. With $U_2(t) = \frac{1}{2}\varpi_2^2(t)$ it follows from (18) that

$$\begin{aligned}\dot{U}_2(t) &= \varpi_2(t)\,\dot{\varpi}_2(t)\\ &= \varpi_2(t)\left(\dot{\varphi}_2(t)\,e_2(t) + \varphi_2(t)\,\dot{e}_2(t)\right)\\ &= \frac{\dot{\varphi}_2(t)}{\varphi_2(t)}\varpi_2^2(t) - \varphi_2(t)k_2(t)\varpi_2^2(t)\\ &\quad + \varphi_2(t)\varpi_2(t)\left(c_1 + c_2 y_2(t) + \Delta_2(t) - \Delta_1(t) + e_3(t)\right)\\ &\quad + \varphi_2(t)\varpi_2(t)\left(1 + 2\varpi_1^2(t)k_1(t)\right)k_1(t)\dot{\varpi}_1(t).\end{aligned} \tag{34}$$

By Step 3 it follows that k_1 is bounded on $t \in [0, t_f)$. Furthermore, $|e_3(t)| < 1/\varphi_3(t)$ and ϖ_1, $\dot{\varpi}_1$, $y_2, \Delta_1, \Delta_2, \varphi_2, \dot{\varphi}_2$ are bounded on $[0, t_f)$, hence there exists a constant $C_2 > 0$ satisfying

$$\begin{aligned}&\frac{|\dot{\varphi}_2(t)|}{\varphi_2^2(t)} + c_1 + c_2|y_2(t)| + |\Delta_2(t)| + |\Delta_1(t)| + |e_3(t)|\\ &+ \left(1 + 2\varpi_1^2(t)k_1(t)\right)k_1(t)|\dot{\varpi}_1(t)| \le C_2.\end{aligned} \tag{35}$$

Invoking $|\varpi_2(t)| < 1$ we thus obtain

$$\dot{U}_2(t) \le \varphi_2(t)|\varpi_2(t)|\left(-k_2(t)|\varpi_2(t)| + C_2\right) \tag{36}$$

and with a similar argument as in Step 3 it can be shown that k_2 is bounded on $[0, t_f)$.

Step 5: We show that k_3 is bounded on $[0, t_f)$. To this end, we substitute (14) into (19), yielding

$$\begin{aligned}\dot{e}_3(t) = &-c_5 k_3(t)\frac{\varpi_3(t)}{\varphi_3(t)} - z_{h_{ref}}^{(4)}(t) + \frac{d}{dt}\left(k_2(t)\,\varpi_2(t)\right)\\ &+ c_3 + c_4 y_2(t) + \Delta_3(t)\end{aligned} \tag{37}$$

Define $U_3(t) = \frac{1}{2}\varpi_3^2(t)$ and calculate

$$\begin{aligned}\dot{U}_3(t) &= \varpi_3(t)\,\dot{\varpi}_3(t)\\ &= \varpi_3(t)\left(\dot{\varphi}_3(t)\,e_3(t) + \varphi_3(t)\,\dot{e}_3(t)\right)\\ &= -c_5 k_3(t)\varpi_3^2(t) + \frac{\dot{\varphi}_3(t)}{\varphi_3(t)}\varpi_3^2(t)\\ &\quad + \varpi_3(t)\,\varphi_3(t)\left(-z_{h_{ref}}^{(4)}(t) + c_3 + c_4 y_2(t) + \Delta_3(t)\right)\\ &\quad + \varpi_3(t)\,\varphi_3(t)\left(1 + 2\varpi_2^2(t)k_2(t)\right)k_2(t)\dot{\varpi}_2(t).\end{aligned} \tag{38}$$

From Step 4 we find that k_2 is bounded on $[0, t_f)$. Because of $|e_3(t)| < 1/\varphi_3(t)$ and boundedness of ϖ_2, $\dot{\varpi}_2$, $y_2, \Delta_3, \varphi_3, \dot{\varphi}_3, z_{h_{ref}}^{(4)}$ on $[0, t_f)$ it follows that there exists $C_3 > 0$ such that

$$\begin{aligned}&\varphi_3(t)\Big(\frac{|\dot{\varphi}_3(t)|}{\varphi_3^2(t)} + \left|z_{h_{ref}}^{(4)}(t)\right| + c_3 + c_4|y_2(t)|\\ &+ |\Delta_3| + \left(1 + 2\varpi_2^2(t)k_2(t)\right)k_2(t)|\dot{\varpi}_2(t)|\Big) \le C_3.\end{aligned} \tag{39}$$

Invoking $|\varpi_3(t)| < 1$ we thus obtain

$$\dot{U}_3(t) \le |\varpi_3(t)|\left(-c_5 k_3(t)|\varpi_3(t)| + C_3\right) \tag{40}$$

and with a similar argument as in Step 3 it can be shown that k_3 is bounded on $[0, t_f)$.

Step 6: We show that $t_f = \infty$. Assuming $t_f < \infty$ it follows from Steps 2–5 that the closure of the graph of $(y_0, \ldots, y_3)$ is a compact subset of D_4, which contradicts the findings of Step 1. Therefore, $t_f = \infty$. ■

Note that the determination of the funnel boundary $\bar{\rho}_0(t)$ is pre-established based on the positional accuracy criteria for the considered maneuvering flight mission. In contrast, $\bar{\rho}_i(t)$ $(i = 1, 2, 3)$ represent adjustable parameters utilized to achieve the overall control objective by expanding or narrowing the permissible range of $e_i(t)$ $(i = 1, 2, 3)$. The control algorithm exhibits divergence when $e_i(t) = \bar{\rho}_i(t)$, which leads to $\varpi_i(t) = 1$, and consequently, $k_i(t) = \frac{1}{1-\varpi_i{}^2(t)}$ tends towards infinity. Particularly during the maneuvering phases, such as BC, DE, FG (as depicted in Fig. 4), errors close to their respective funnel boundary become more likely. This phenomenon primarily arises due to the rapid changes of the reference trajectory during maneuvers, which reduces the gap between the error and its corresponding funnel boundary. This exacerbates the likelihood of the gain parameter $k_i(t)$ approaching infinity, ultimately leading to instability of the closed-loop system.

Further note that the work [26] also employs funnel control techniques to solve the tracking problem with prescribed transient behavior for RVs. However, the controller there requires additional design parameters which need to be sufficiently large, but it is not known a priori how large they must be chosen. In the present paper, we avoid this problem by introducing a novel error variable form as in (13). This seems advantageous for practical engineering.

IV. SIMULATION

In this section, we illustrate the performance of the funnel controller (14) by considering the lateral action of a RV with constant speed $V = 5\,\text{Mach}$ at a height of 20 km. The initial states of the RV and the values of the geometric system parameters are shown in Table I. In practical engineering applications, input constraints are always present. Therefore, although such constraints are not considered in the theoretical treatment in Theorem 1, we incorporated them in the simulation such that the actual control input is $\text{sat}(u(t))$, where $\text{sat}(v) = v$ for $|v| \le 40$ and $\text{sat}(v) = \text{sgn}(v)40$ for $|v| > 40$. The simulation was performed in MATLAB (solver: ODE45, default tolerances).

As for the maneuvering reference trajectory, an extensively used Dubins trajectory is selected as the planning path, shown in Fig. 4, where θ_j $(j = BC, DE, FG)$ and R_j are the turning radius and central angles, respectively. The coordinates of the starting point, turning points and end point are $A\,(0, 450\text{m})$, $B\,(12\text{km}, 50\text{m})$, $C\,(15\text{km}, 0)$, $D\,(24\text{km}, 0)$, $E\,(27\text{km}, 50\text{m})$, $F\,(30\text{km}, 150\text{m})$, $G\,(35\text{km}, 260\text{m})$ and $H\,(48.53\text{km}, -200\text{m})$. The time consumed per period is calculated by $t_i = \frac{\bar{l}_i}{V}$ $(i = AB, CD, EF, GH)$ through straight regions and $t_j = \frac{\widehat{l}_j}{V} = \frac{\theta_j R_j}{V}$ $(j = BC, DE, FG)$ in turning areas. Since the proposed performance funnel is time-triggered based on the planning path, the triggered times are set in accordance with the time points of the

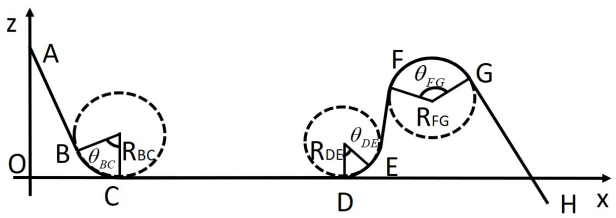

Fig. 4. Planning trajectory for RV

reference trajectory, resulting in $p = 3$. Thus the parameters of the funnel boundary function of the form (11) are chosen as in Table II.

In order to comprehensively verify the effectiveness of our proposed algorithm, we study three cases in the simulations, that is, the Nominal Case (without disturbances), Case 1 (with disturbances $\Delta_i(t)$ $(i = 0, 1, 2, 3)$ and aerodynamic parameters biased +10%) and Case 2 (with disturbances $\Delta_i(t)$ $(i = 0, 1, 2, 3)$ and aerodynamic parameters biased -10%), where the involved aerodynamic parameters are $c_z^\alpha, c_z^\beta, c_z^0, c_M^\alpha, c_M^\beta, c_M^{\delta_y}, c_M^0$. As disturbances we choose $\Delta_0(t) = \frac{5}{57.3}\sin\left(\frac{\pi}{4}t\right)$, $\Delta_1(t) = \frac{0.2}{57.3}\sin\left(\frac{\pi}{4}t\right)$, $\Delta_2(t) = \frac{2}{57.3}\sin\left(\frac{\pi}{4}t\right)$, $\Delta_3(t) = \frac{10}{57.3}\sin\left(\frac{\pi}{4}t\right)$.

The results are depicted in Figs. 5–11. The tracking error e_0 and the auxiliary errors e_1, e_2, e_3 are shown in Figs. 5–8. It is found that e_3 is more sensitive to maneuvering than e_0, where a slight jump appears near each trigger time. In all three cases, every error e_i $(i = 0, 1, 2, 3)$ is kept within its respective funnel through the whole process. The control input, represented by the rudder angle, is shown in Fig. 9. It is evident that the control input exhibits a peak at both the starting and the turning point, leading to control saturation due to the constraints imposed on the input. In accordance with Theorem 1, this phenomenon exemplifies the means by which the proposed control algorithm endeavors to mitigate the chances of errors transgressing the funnel boundaries to the greatest extent possible. Though input saturation is not covered by Theorem 1, it is unmistakable that the controller demonstrates exceptional performance under these input constraints. Nonetheless, it remains crucial to recognize that achieving the optimal performance of the control algorithm necessitates to comprise input constraints. Future research should aim to establish the theoretical guarantees for such a performance.

Fig. 10 shows the deflection angle, sideslip angle, yaw angle and yaw rate to illustrate that all variables in the closed-loop system are bounded in all three cases. The tracking maneuver reference trajectory is shown in Fig. 11 together with the output signals generated under control. Although the performance of the vehicle in the continuous large maneuver segment is not as good as that in the single maneuver segment, we observe a decent tracking performance overall. Furthermore, the presented simulations demonstrate the inherent robustness properties of the control algorithm.

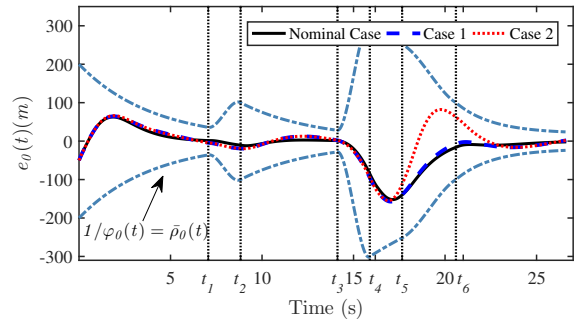

Fig. 5. Response of tracking error $e_0(t)$.

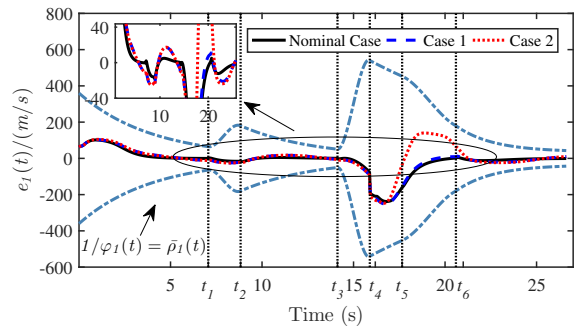

Fig. 6. Response of error $e_1(t)$.

However, we like to note that in this example the theoretical condition (15) from Theorem 1 is not satisfied, yet the controller still works. This shows that the assumptions of Theorem 1 are quite conservative and further research is necessary to relax them. A thorough inspection of the proof of Theorem 1 reveals that the conservativeness of condition (15) is due to the utilization of the mean value theorem and avoiding it could lead to a weaker condition.

V. CONCLUSION

In this paper, we have devised a funnel-based tracking control algorithm to ensure the prescribed performance of tracking errors in reentry vehicles operating in the presence of disturbances during maneuvering flight missions. Our simulation results conclusively demonstrate that the proposed control method effectively stabilizes

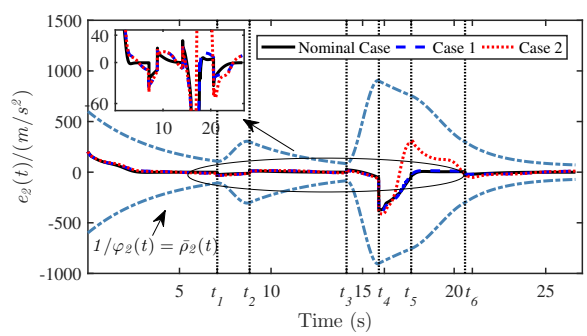

Fig. 7. Response of error $e_2(t)$.

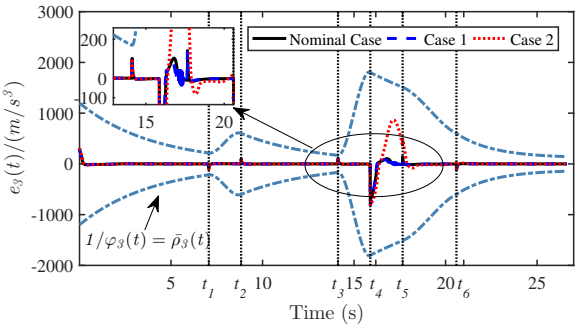

Fig. 8. Response of error $e_3(t)$.

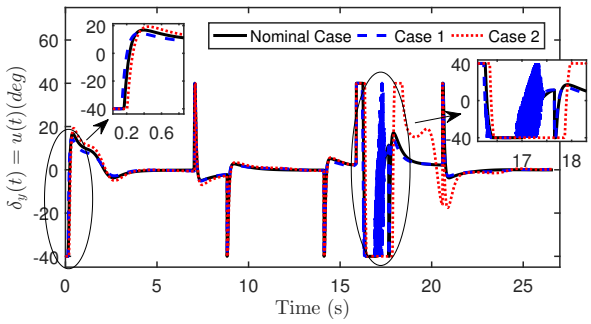

Fig. 9. Response of control input $\delta_y(t) = u(t)$.

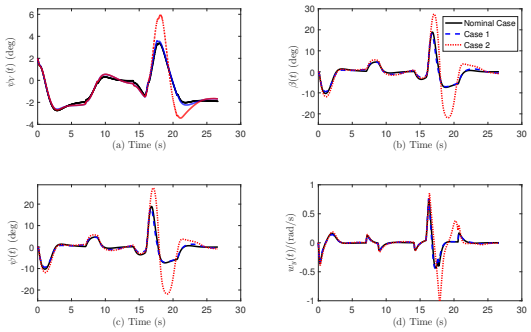

Fig. 10. Response : (a) $\psi_V(t)$, (b) $\beta(t)$, (c) $\psi(t)$, (d) $\omega_y(t)$.

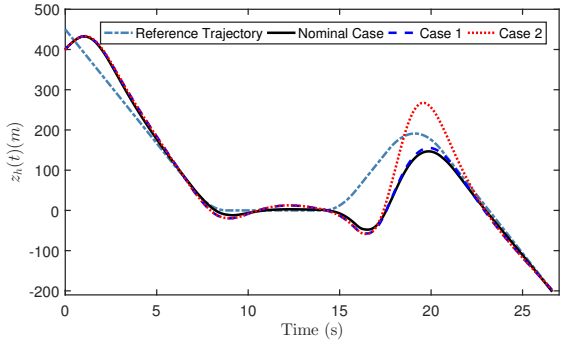

Fig. 11. Response of $z_h(t)$ and $z_{h_{ref}}(t)$.

TABLE I

Geometric parameters and initial state of RV

Variables	Value	Variables	Value
m (kg)	1200	$z_h(0)$ (m)	400
S (m^2)	1.3	$\psi_V(0)$ (rad)	2/57.3
l (m)	1.7	$\psi(0)$ (rad)	4/57.3
J_y ($kg \cdot m^2$)	8110	$\omega_y(0)$ (rad/s)	0.035
α (rad)	5/57.3	$\beta(0)$	2/57.3
c_z^α	0	c_z^β	0.1852
c_z^0	-0.018714	c_M^α	-0.1
c_M^β	2.1335	$c_M^{\delta_y}$	5.1588
c_M^0	0.18979	$\bar{q}$	3711.93329

TABLE II

Parameters of the proposed funnel boundary

Variables	Value
$\bar{\rho}_0(t)$(m)	$\bar{\rho}_{0,1}^0 = 200$, $\bar{\rho}_{0,2}^0 = 100$, $\bar{\rho}_{0,3}^0 = 300$, $\bar{\rho}_{0,4}^0 = 100$, $\bar{\rho}_{0,1}^\infty = 2$, $\bar{\rho}_{0,2}^\infty = 2$, $\bar{\rho}_{0,3}^\infty = 2$, $\bar{\rho}_{0,4}^\infty = 10$, $l_{0,1} = 0.25$, $l_{0,2} = 0.25$, $l_{0,3} = 0.5, l_{0,4} = 0.1$
$\bar{\rho}_1(t)$(rad)	$\bar{\rho}_1(t) = 1.8\bar{\rho}_0(t)$
$\bar{\rho}_2(t)$(rad)	$\bar{\rho}_2(t) = 3\bar{\rho}_0(t)$
$\bar{\rho}_3(t)$(rad/s)	$\bar{\rho}_3(t) = 6\bar{\rho}_0(t)$

all variables within the closed-loop system and consistently maintains the predetermined performance criteria throughout the entire trajectory, even during rapid trajectory maneuvers. This successfully validates the applicability and effectiveness of the proposed time-triggered, non-monotonic funnel boundary under maneuvering mission conditions. Future research will focus on the relaxation of the conditions of Theorem 1 as well as their extension to the presence of input constraints. To this end, the recent results in [32] might be a starting point.

REFERENCES

[1] Han T, Hu Q, Shin H S, et al. Incremental twisting fault tolerant control for hypersonic vehicles with partial model knowledge. IEEE Transactions on Industrial Informatics, 2021, 18(2): 1050-1060.

[2] Chai R, Tsourdos A, Savvaris A L, et al. Trajectory planning for hypersonic reentry vehicle satisfying deterministic and probabilistic constraints. Acta Astronautica, 2020, 177: 30-38.

[3] Shen G, Xia Y, Zhang J, et al. Adaptive super-twisting sliding mode altitude trajectory tracking control for reentry vehicle. ISA Transactions, 2022.

[4] Mehra R. A comparison of several nonlinear filters for reentry vehicle tracking. IEEE Transactions on Automatic Control 1971, 16(4):307-319.

[5] Peng Z, Wang D, Li T, et al. Output-feedback cooperative formation maneuvering of autonomous surface vehicles with connectivity preservation and collision avoidance. IEEE Transactions on Cybernetics, 2019, 50(6): 2527-2535.

[6] Yao P, Wang H, Su Z. Real-time path planning of unmanned aerial vehicle for target tracking and obstacle avoidance in complex dynamic environment. Aerospace Science and Technology, 2015, 47: 269-279.

[7] Zhang R, Zong Q, Zhang X, et al. Game of Drones: Multi-UAV Pursuit-Evasion Game With Online Motion Planning by Deep Reinforcement Learning. IEEE Transactions on Neural Networks and Learning Systems, 2022.

[8] Yang H I, Zhao Y J. Trajectory planning for autonomous aerospace vehicles amid known obstacles and conflicts. Journal of Guidance, Control, and Dynamics, 2004, 27 (6): 997-1008.

[9] Pounds P E, Bersak D R, Dollar A M. Stability of small-scale UAV helicopters and quadrotors with added payload mass under PID control. Autonomous Robots, 2012, 129-142.

[10] Elmokadem T, Zribi M, Youcef-Toumi K. Trajectory tracking sliding mode control of underactuated AUVs. Nonlinear Dynamics, 2016, 84(2): 1079-1091.

[11] Cho G R, Li J H, Park D, et al. Robust trajectory tracking of autonomous underwater vehicles using back-stepping control and time delay estimation. Ocean Engineering, 2020, 201: 107131.

[12] Beikzadeh H, Liu G. Trajectory tracking of quadrotor flying manipulators using L1 adaptive control. Journal of the Franklin Institute, 2018, 355(14): 6239-6261.

[13] Zuo Z, Ru P. Augmented L-1 adaptive tracking control of quadrotor unmanned aircrafts. IEEE Transactions on Aerospace and Electronic Systems, 2014, 50 (4): 3090-3101.

[14] Chai R, Tsourdos A, Savvaris A, et al. Solving constrained trajectory planning problems using biased particle swarm optimization. IEEE Transactions on Aerospace and Electronic Systems, 2021, 57(3): 1685-1701.

[15] Chai R, Tsourdos A, Savvaris A, et al. Six-DOF spacecraft optimal trajectory planning and real-time attitude control: a deep neural network-based approach. IEEE Transactions on Neural Networks and Learning systems, 2019, 31(11): 5005-5013.

[16] Mu C, Ni Z, Sun C, et al. Air-breathing hypersonic vehicle tracking control based on adaptive dynamic programming. IEEE Transactions on Neural Networks and Learning systems, 2016, 28(3): 584-598.

[17] Peng Z, Wang J. Output-feedback path-following control of autonomous underwater vehicles based on an extended state observer and projection neural networks. IEEE Transactions on Systems, Man, and Cybernetics: Systems, 2017, 48(4): 535-544.

[18] Bechlioulis C P, Rovithakis G A. Robust adaptive control of feedback linearizable MIMO nonlinear systems with prescribed performance. IEEE Transactions on Automatic Control, 2008, 53(9): 2090-2099.

[19] Bechlioulis C P, Rovithakis G A. Adaptive control with guaranteed transient and steady state tracking error bounds for strict feedback systems. Automatica, 2009, 45(2): 532-538.

[20] Guo Z, Oliveira T R, Guo J, Wang Z. Performance-guaranteed adaptive asymptotic tracking for nonlinear systems with unknown sign-switching control direction. IEEE Transactions on Automatatic Control, 2023, 68 (2): 1077-1084.

[21] Ilchmann A, Ryan E P, Sangwin C J. Tracking with prescribed transient behaviour. ESAIM: Control, Optimisation and Calculus of Variations, 2002, 7: 471-493.

[22] Berger T, Le H H, Reis T. Funnel control for nonlinear systems with known strict relative degree. Automatica, 2018, 87: 345-357.

[23] Berger T, Ilchmann A, Ryan E P. Funnel control of nonlinear systems. Mathematics of Control, Signals, and Systems, 2021, 33: 151-194.

[24] Berger T, Rauert A L. Funnel cruise control. Automatica, 2020, 119: 109061.

[25] Berger T, Puche M, Schwenninger F L. Funnel control for a moving water tank. Automatica, 2022, 135: 109999.

[26] Gu X, Guo J, Guo Z, et al. Performance improvement-oriented reentry attitude control for reusable launch vehicles with overload constraint. ISA Transactions, 2022, 128: 386-396.

[27] Bu X. Guaranteeing prescribed performance for air-breathing hypersonic vehicles via an adaptive non-affine tracking controller. Acta Astronautica, 2018, 151: 368-379.

[28] Bu X, Wei D, Wu X, et al. Guaranteeing preselected tracking quality for air-breathing hypersonic non-affine models with an unknown control direction via concise neural control. Journal of the Franklin Institute, 2016, 353(13): 3207-3232.

[29] Chai R, Tsourdos A, Savvaris A L, et al. Trajectory planning for hypersonic reentry vehicle satisfying deterministic and probabilistic constraints. Acta Astronautica, 2020, 177: 30-38.

[30] Hu G, Guo J, Guo Z, et al. ADP-based intelligent tracking algorithm for reentry vehicles subjected to model and state uncertainties. IEEE Transactions on Industrial Informatics, 2022.

[31] Ilchmann A, Ryan E P. Performance funnels and tracking control. International Journal of Control, 2009, 82(10): 1828-1840.

[32] Berger T. Input-constrained funnel control of nonlinear systems. Submitted for publication, preprint available on arXiv: https://arxiv.org/abs/2202.05494.

Zongyi Guo (Member, IEEE) received the M.E. and Ph.D. degrees in navigation guidance and control from Northwestern Polytechnical University, Xi'an, China, in 2013 and 2017, respectively. He is currently an Associate Researcher of Navigation Guidance and Control with the School of Astronautics, Northwestern Polytechnical University, Xi'an, China. His research interests include robust control, coupling control, learning-based control with their applications to aerospace systems. He serves as an Associate Editor for Measurement and Control.

Xiyu Gu received B.S. and M.S. degrees from Northwestern Polytechnical University, Xi'an, China, in 2019 and 2022, respectively. She is currently working toward the Ph.D. degree with the Department of Information Engineering (DEI) from the University of Padova, Padua, Italy. Her research interests include prescribed performance control, optimal control with their applications in aerospace systems and network systems.

Yonglin Han received the B.E. degree in automation, in 2022, from Chang'an University, Xi'an, China. He is currently working toward the M.E. degree in electronic information with the School of Astronautics, Northwestern Polytechnical University, Xi'an, China. His research interests include guidance and control for vehicles and prescribed performance control.

Jianguo Guo received the B.E. and M.E. degrees in applied mathematics, from Henan Normal University, Xinxiang, China, in 1998 and 2001, respectively, and the Ph.D. degree in navigation guidance and control from Northwestern Polytechnical University, Xi'an, China, in 2005. He is currently the Director of the Institute of Precision Guidance and Control and a Full Professor of Navigation Guidance and Control with the School of Astronautics, Northwestern Polytechnical University. His research interests include guidance and control for flight vehicles, sliding mode control and robust control.

Thomas Berger was born in Germany in 1986. He received his B.Sc. (2008), M.Sc. (2010), and Ph.D. (2013), all in Mathematics and from Technische Universität Ilmenau, Germany. From 2013 to 2018 Dr. Berger was a postdoctoral researcher at the Department of Mathematics, Universität Hamburg, Germany. Since January 2019 he is a Juniorprofessor at the Institute for Mathematics, Universität Paderborn, Germany. His research interest encompasses adaptive control, optimization-based control, differential-algebraic systems and multibody dynamics. For his exceptional scientific achievements in the field of Applied Mathematics and Mechanics, Dr. Berger received the "Richard-von-Mises Prize 2021" of the International Association of Applied Mathematics and Mechanics (GAMM). He further received several awards for his dissertation, including the "2015 European Ph.D. Award on Control for Complex and Heterogeneous Systems" from the European Embedded Control Institute and the "Dr.-Körper-Preis 2015" from the GAMM. He serves as an Associate Editor for Mathematics of Control, Signals, and Systems, the IMA Journal of Mathematical Control and Information and the DAE Panel, and as a Review Editor for Frontiers in Control Engineering.